Effects of Climate Change on Landslide Slope Stability and Case Studies

Shiro Ota, Masafumi Okawara, Nobuo Sakakibara, and Takamasa Yamaji

Abstract In recent years, disasters caused by torrential rains and floods that exceed the planned scale are occurring in Japan due to climatic change. In response to it, Japan has been improving and reinforcing existing infrastructure to withstand more severe disasters. For example, in river projects, widening river width through channel excavation to increase flow capacity, and in road projects, lane widening and reinforcement of existing embankments to enhance the traffic network during disasters are occurring. At these project sites, there is concern that artificial topographic modification (changes in stress conditions due to excavation and embankment), which was conducted as a countermeasure, will affect potential weak surfaces in the ground, which, combined with the effects of increased rainfall caused by climate change, will destabilize the existing slopes and cause new slope changes (Kaneko in A collection of papers from the China Branch of Geotechnical Society, pp.161–168, 2018). In this wise, the demand for the assessment of landslide slope stability associated with increased rainfall caused by climate change and artificial modification is increasing; in this study, we examined a method for the assessment of landslide slope stability that takes into account the change in the strength of the slip surface associated with increased rainfall and artificial modification targeting a landslide area near a planned site for excavation of a river channel.

Keywords Climate change · Landslide · Slope stability analysis

S. Ota (✉)
Kawasaki Geological Engineering Co., Ltd. Planning and Technical Headquarters, Minato-ku, Tokyo, Japan
e-mail: ohtas@kge.co.jp

M. Okawara
Faculty of Science and Engineering, Iwate University, Morioka, Iwate Prefecture, Japan

N. Sakakibara
Kawasaki Geological Engineering Co., Ltd. North Japan Branch, Miyagino-ku, Sendai, Miyagi Prefecture, Japan

T. Yamaji
Kawasaki Geological Engineering Co., Ltd. Kyusyu Branch, Hakata-ku, Fukuoka, Fukuoka Prefecture, Japan

1   Introduction

In addition to the occurrence of new landslide disasters caused by rainfall increased due to climate change, there are landslides occurred that have stabilized due to the implementation of countermeasures and have changed in the past and are now inactive. Landslide reactivation is feared. To predict and assess the risk of slope instability associated with increased rainfall properly, it is necessary to estimate the increase and distribution of pore water pressure on slopes associated with increased rainfall accurately. However, pore water pressure on slopes is often determined based on groundwater level observation data in Japan, and if there is no record of heavy rainfall during the observation period, it may not be possible to estimate properly the pore water pressure for increased rainfall. Therefore, in this study, we examined a method for estimating the increase in pore water pressure due to rainfall above the observed rainfall in a landslide facing a river using seepage flow analysis.

In Japan, road widening (excavation) and river widening to prevent river flooding are being promoted as measures to create a country resilient to climate change. It is often accompanied by excavation and embankment modification, which causes the stress state of the slope to change, the strength of the slip surface to decrease due to the progress of displacement and water absorption expansion, and the slope to become unstable. Therefore, in this study, a method for setting slip surface strength considering water absorption expansion by indoor shear test and a method for slope stability evaluation by 3D stability analysis were investigated.

2   Outline of the Target Landslide

2.1   Outline of the Landslide

In the target area, when a landslide occurred in Block B (length 126 m, width 138 m) shown in Fig. 1 during the construction to widen the river in the past, the head soil removal work was conducted. In the adjacent Block A (length 380 m, width 295 m), no landslide deformation was observed in visual and field observations, but two water collecting wells were installed to improve safety and maintain stability. However, the widening of the river was required to increase the water flow of the river, and the countermeasure was pending issue.

As shown in Fig. 2, Block A of the landslide shows a characteristic landslide topography in which the bedrock of the monoclinal structure (cuesta landform) bent in the middle and rose at the end. Since the crushing of the bedrock consisting of the landslide mass was localized, differentiation of the landslide block was not approved, and no clear deformation was observed in the field monitoring, it is now considered to be a primary landslide in an inactive condition. The geology of the subject area consists of Neogene Miocene tuff (mudstone, tuff, and alternating layers of tuffaceous
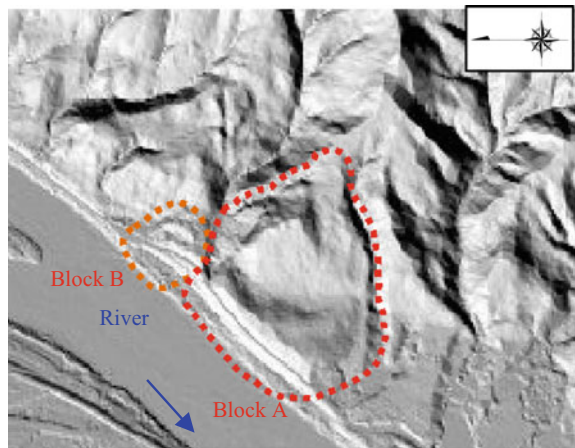
Fig. 1 Bird's-eye view of topography

Fig. 2 Schematic cross-sectional view
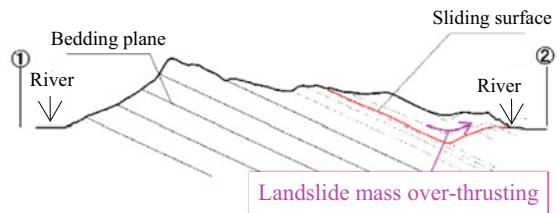
Fig. 3 Topographic shadow diagram

sandstone and mudstone) distributed with north–south strike and gentle west-dipping monoclinic structure in the west area and steep cliffs in the east area, and the direction of the movement is 25° oblique to the river direction (Figs. 3 and 4).
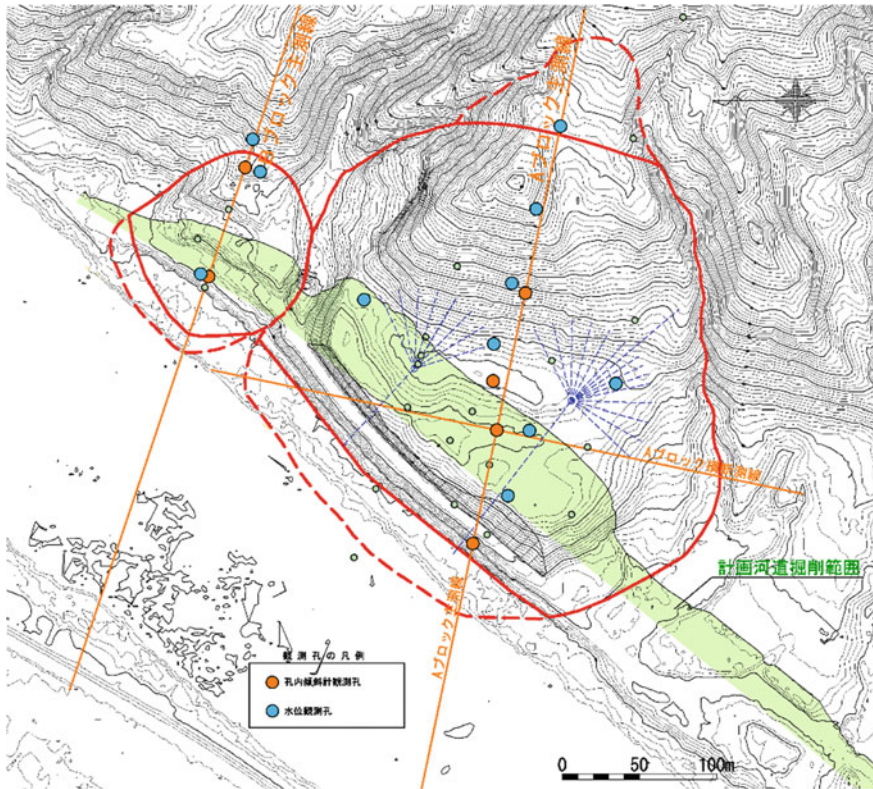
**Fig. 4** Excavation plan for landslide terminus

2.2 Recognition of Slip Surfaces

A geological survey was conducted to identify the geologic stratigraphy and the
inclination direction of the geologic boundary, and the clay layer was extracted as
a slip surface. Then, based on the presence or absence of mirror skin and striations,
and the inclination angle, the slip surface was defined by the method shown in Photo
1 and Fig. 5.

A cross-sectional view of the landslide is shown in Fig. 5. The slip surface was
estimated to slope down to the riverside from the head to the bend and to ride up to the
riverside from the bend to the riverside. At the foot of the landslide, an unconsolidated
sand and gravel layer of the old riverbed was observed directly under the moving
soil mass, and from its distribution range, the amount of movement caused by the
landslide was estimated to be 80 m or more. On the other hand, since the crushing
of the mobile soil mass was limited along the slip surface from the bend to the head,
the majority of the mobile soil mass was massive bedrock with few cracks, and no
subsurface movement was confirmed by dynamic monitoring, it was presumed to be

Photo 1 Slickensides and striations
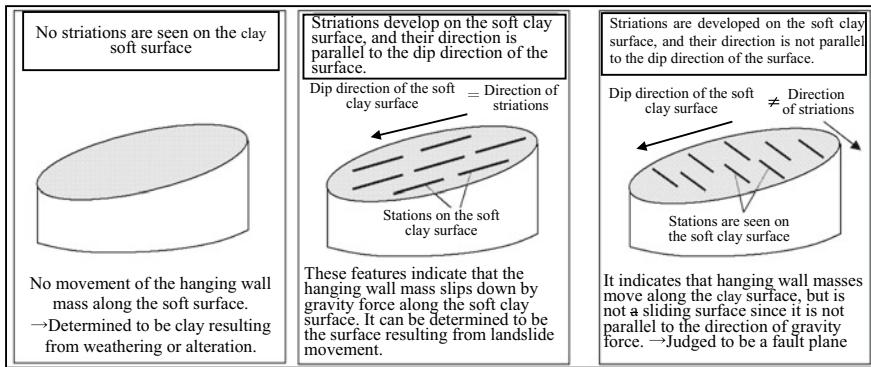
**Fig. 5** Conceptual diagram of landslide surface certification

a primary slip caused by external factors such as an earthquake with large movement, and it was judged to be in a state of arrested movement at present (Fig. 6).

3 Slip Surface Strength from Cyclic Box-Shear Tests

3.1 Test Conditions

In this study, the following innovations were used to determine the strength of the slip surface in cyclic one-sided shear tests.

Fragile areas around the slip surface were crushed and slurried, and the specimens (6 cm diameter and 2 cm high) were compacted under a pressure equivalent to the thickness of the overburden. The specimens were then unloaded at a load equivalent
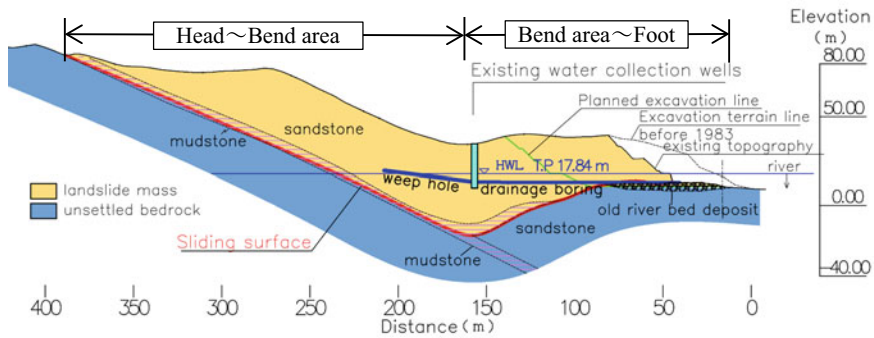
Fig. 6 Schematic diagram of landslide cross-section

to the height of the river excavation (10 m), dried at 60 °C for 24 h, and subjected to shear tests after water absorption. The residual strength was determined as the fully softened strength when recompacted by residual soil or when the slip surface was completely separated due to high shear displacement [2]. For comparison, shear tests were also carried out at natural water content.

3.2 Tests Results

The shear strength of several specimens was compared under natural water content conditions and underwater absorption and dewatering conditions. The test results in underwater absorption and dewatering conditions showed that the shear resistance angle Φ decreased by 1° to 2° due to the increased saturation state caused by water absorption. The variation in both the fully softened strength and residual strength was reduced because the saturation state became constant due to water absorption. Based on the test averages of all 15 sample's underwater absorption and dewatering conditions, the degrees were set as follows: fully softened strength: c = 21.8 (kN/m^2), ϕ = 15.2°; residual strength: c = 0.0 (kN/m^2), ϕ = 13.8° (Table 1).

3.3 Slip Surface Strength Zoning

In the practice of stability assessment of landslide slopes in Japan, shear strength (c, Φ) of the slip surface for 2D stability analysis using the limit equilibrium method is rarely obtained from soil tests. The adhesion force (c) is obtained from the maximum thickness of the landslide soil mass, and the shear resistance angle Φ is set by back-calculating the initial safety factor Fs = 0.95 to 1.05 from the existing topography depending on the situation. However, since the properties and strength are expected

Table 1 Repeated cyclic box-shear tests results

Statistics	Forced water absorption state			
	Fully softened strength		Residual strength	
	Cohesion	Angle of shear resistance	Cohesion	Angle of shear resistance
	$c(kN/m^2)$	$\varphi(°)$	$c(kN/m^2)$	$\varphi(°)$
Maximum value	50.9	27.2	0.0	24.7
Minimum value	0.0	10.9	0.0	10.6
Median value	17.2	14.2	0.0	13.0
Average value	21.8	15.2	0.0	13.8
Number of test	15		15	

to differ depending on the location of the slip surface of the landslide in question, and there is concern that the strength may decrease with excavation, zoning according to soil test results and the properties of the slip surface [3] is appropriate.

Definitions of Shear Strength Obtained from Soil Tests

Fully softened strength. It is the peak strength obtained by regular consolidation from kneading and recompressing clay and the strength of an active slip surface in which rocks and clays were destroyed by an initial landslide and released from the effects of previous consolidation or reconsolidated by overburden loads for some time after activity was stopped.

Residual strength. This is the minimum shear strength when a large shear displacement has been applied, and a residual condition has been reached, such as when a slickenside is formed on the slip surface.

Slip Surface Strength Zoning Results

From the head to the bend in the landslide mass, the slip surface is straight and completely clayed by the large shear displacement during the initial landslide. The strength of the slip is judged to be equivalent to "residual strength" because a slickenside and striations are observed. The area from the bend to the end of the landslide shows hard clay mixed with gravel, which indicates that the moving soil mass rode up on the immovable ground and riverbed during the initial landslide and was crushed and clayed, and then reconsolidated by soil overburden load or horizontal compressive force. Although slickensides and striations are recognized in some parts, no clear separation surface is recognized as a whole, and therefore, its strength is judged to be equivalent to "full softened strength" (Fig. 7 and Tables 2 and 3).

3D stability analysis [4] was used to determine the factor of safety of the landslide slope at the highest observed water level. For the case of total residual strength, Fs = 0.93, which is inconsistent with the absence of landslide movement in Block A. For the total complete softening strength, Fs = 1.34, which is inconsistent with the situation where Block B collapsed due to past river channel excavation and Block A has no margin. Compared to the safety factor when the strength is set by the inverse
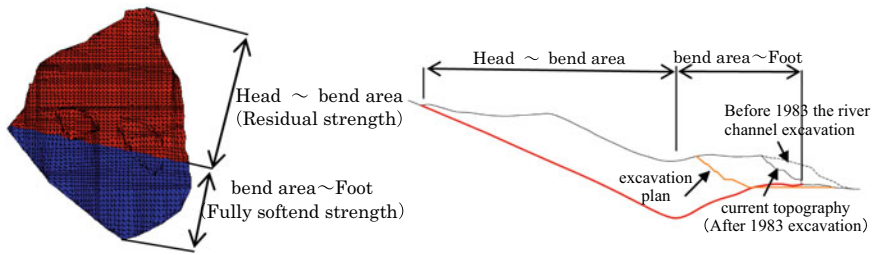
Fig. 7 Planar and longitudinal sectional maps of slip surface strength

method, the safety factor is the same for the current topography and before the past excavation, but the safety factor is calculated as 10% lower for the future excavation plan due to zoning. It is considered that the zoning set the slip surface strength at the time of excavation to the full softening strength and excavated the area of higher resistance, resulting in a greater degree of reduction in the safety factor. From the above, it is judged that the strength setting by zoning is an appropriate method that reflects the local landslide conditions.

4 Slope Stability Assessment for Inexperienced Heavy Rainfall

4.1 Prediction of Groundwater Level by Quasi-3D Seepage Flow Analysis

Since the landslide in question consists of three permeable zones: the slip surface (impermeable layer), the moving soil mass (permeable layer), and the existing catchment well (highly permeable layer), a quasi-3D seepage flow analysis [5] was applied, which reduced calculation labor while considering the 3D extent of the aquifer and the multiple aquifers. The predictive model was determined by setting the hydraulic conductivity and porosity based on the results of field permeability tests conducted for each formation and then fitting the hydraulic conductivity within the range of the test values so that the error between the calculated and observed water levels during actual rainfall would be within $\pm$ 3 m. The model was then finalized (Figs. 8 and 9).
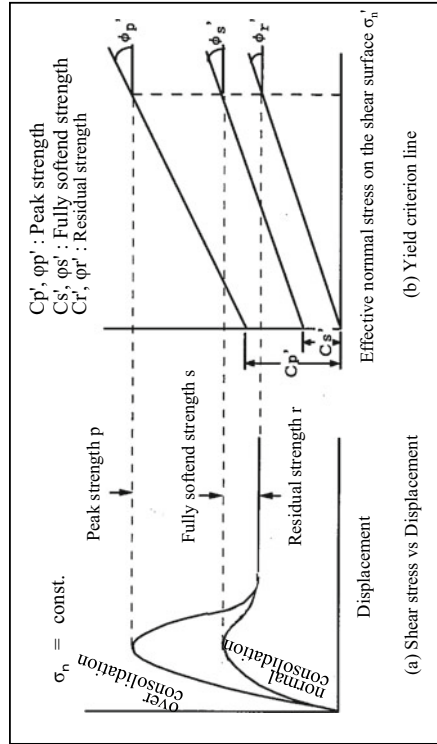
4.2 Evaluation of Slope Stability During Heavy Rainfall

The rainfall waveforms input to the seepage flow analysis were stretched from existing observation waveforms to an arbitrarily set maximum daily rainfall, and rainfall probabilities were calculated using the widely used "Iwai equation" (Fig. 10)

Table 2 Features of the slide surfaces and strength classifications

| Strength classification	Head ~ bend area	Bend area ~ Foot
Photogragh	Residual strength $c = 0.0(kN/m^2)$ $\varphi = 13.8(°)$	Fully softened strength $c = 21.8(kN/m^2)$ $3000\varphi = 15.2(°)$
Soil features	Clay (soft). There are slickensides and slickenlines	Gravel-bearing clay (reconsolidation). There is no slickenside and slickenline

Concept of shear strength obtained from soil tests

(a) Shear stress vs Displacement

(b) Yield criterion line

$\sigma_n = $ const.

over consolidation

normal consolidation

Peak strength p

Fully softend strength s

Residual strength r

Displacement

ϕ_p'

ϕ_s'

ϕ_r'

Effective normal stress on the shear surface σ_n'

Cp', φp' : Peak strength
Cs', φs' : Fully softend strength
Cr', φr' : Residual strength

Cp'

Cs'

Table 3 Safety factor based on 3D stability analysis

Setting method for the strength of the sliding surface	Safety factor based on three-dimensional stability analysis						Remarks
	Before 1983 the river channel excavation		Current topography (After 1983 excavation)		Future excavation (Plan)		
Zoning by the both strength (adopted)	1.37	100%	1.07	100%	0.67	100%	Highest observed groundwater level (Equivalent to 1/60th probability precipitation)
Residual strength all	1.23	90%	0.93	87%	0.58	87%	$c = 0kN/m^2$ $\varphi = 13.8°$
Fully softened strength all	1.69	123%	1.34	125%	0.85	127%	$c = 21.8N/m^2$ $\varphi = 15.2°$
Inverse calculation method (at current topography, Fs = 1.05)	1.38	101%	1.05	98%	0.74	110%	$c = 25kN/m^2$ $\varphi = 11.22°$
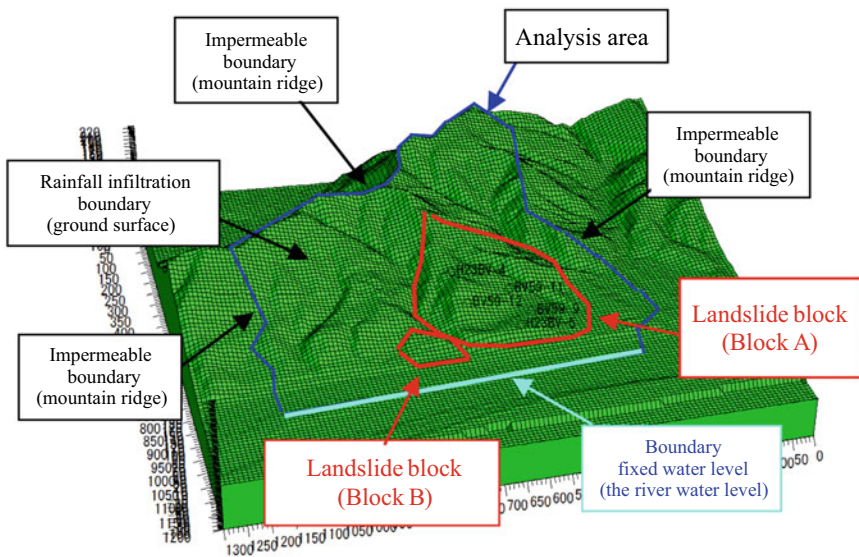
Fig. 8 Schematic diagram of the seepage flow analysis model
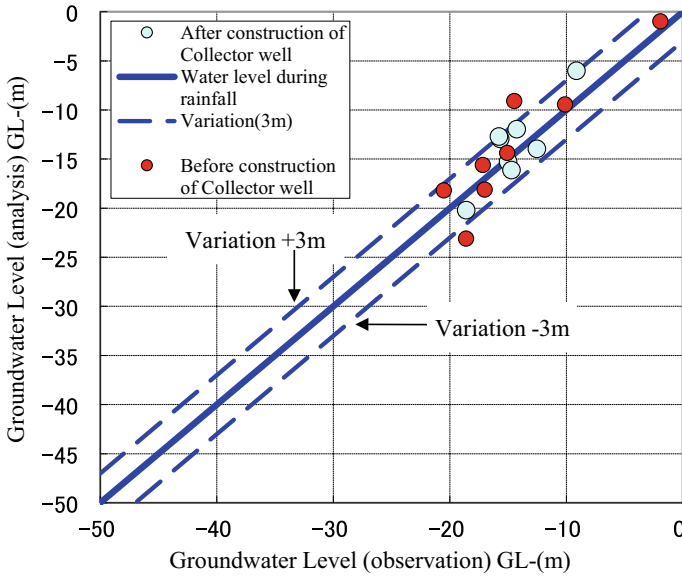
**Fig. 9** Comparison of predicted and measured groundwater levels

[6]. Based on this rainfall waveform, groundwater levels were predicted by quasi-3D seepage flow analysis, and stability was evaluated by 3D stability analysis. This resulted in a predicted critical daily rainfall of 224.7 mm (1/350), which was sufficient to maintain stability (Fig. 11).

The slip factor of safety for existing slopes (Table 4) showed a significant degree of decrease with increasing rainfall, reflecting the increase in the groundwater level of the landslide soil mass as rainfall increases. On the other hand, the safety factor was less than 1.0 in the river widening plan to improve the flow capacity of the river, as shown in Table 3. Therefore, sediment removal works with a safety factor of Fs = 1.05 or higher were considered, and the results of rainfall and safety factors are shown in Table 4. Since most of the landslide soil mass was removed (Fig. 12) and there was little room for the groundwater table to rise, it was determined that there was an upper limit to the decrease in the factor of safety with increasing rainfall and that the stability of the slope could be improved.

Fig. 10 Chart for
calculating probable rainfall
precipitation using the Iwai
method
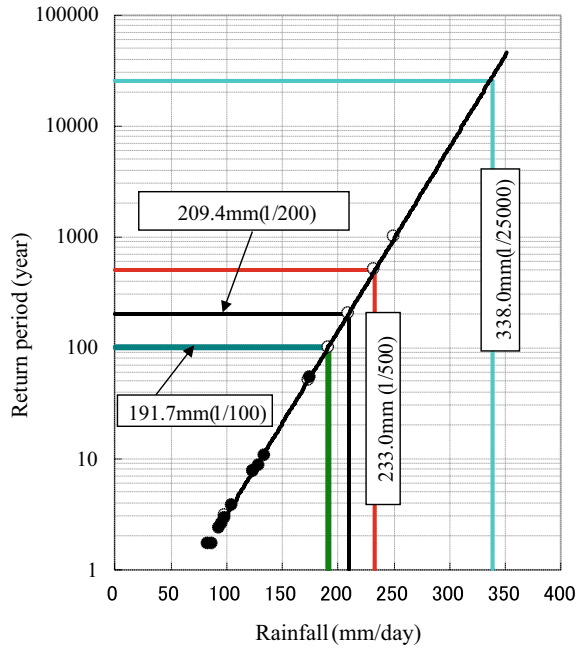
Fig. 11 Chart for
calculating the critical
rainfall that maintains slope
stability
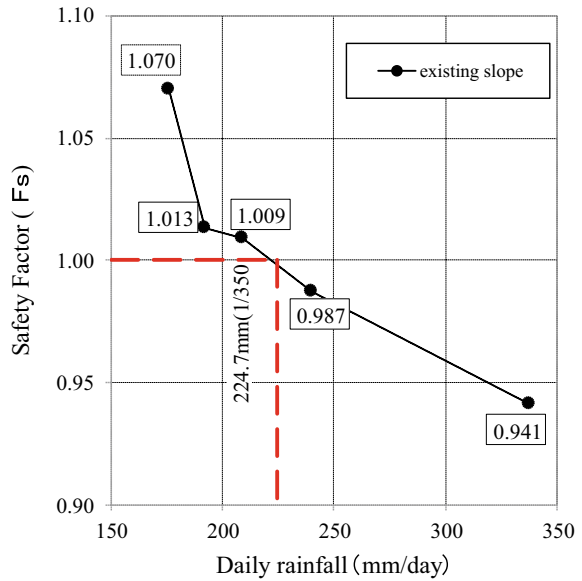
Table 4 Safety rate during heavy rain

Case	Collector well	Safety factor(Fs)				
		176 mm/ day(1/60)	192 mm/ day(1/100)	209 mm/ day(1/200)	233 mm/ day(1/500)	338 mm/ day(1/ 25,000)
Existing slope	2 wells (Existing)	1.070 (Observed water level)	1.013	1.009	*0.987*	*0.941*
River widening and Earth removal work	Ignore effects	–	1.064	1.058	1.051	1.033
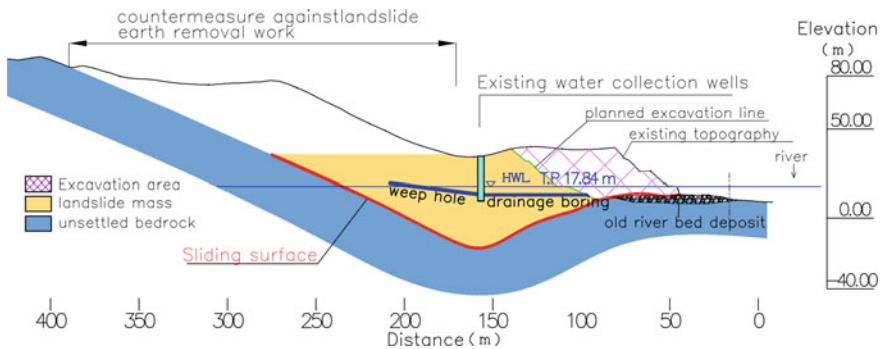
Fig. 12 Landslide prevention work for river widening

5 Conclusion

Several methods based on 2D analysis have been proposed for predicting the stability of landslide slopes with increased rainfall [7], but there are few established examples of 3D analysis combining seepage flow analysis and slope stability analysis. The quasi-3D seepage flow analysis and 3D stability analysis techniques presented in this report were put to practical use in the 1990s and are used, for example, in tunnel construction for the prediction of groundwater impacts associated with excavation and the evaluation of tunnel entrance slope stability. In this study, quasi-3D seepage flow analysis and 3D stability analysis were combined to predict the stability of landslide slopes with increasing rainfall. As the geological composition and distribution of slip surfaces in the target area were well known, modeling of the geological formations and parameter fitting using observation data were relatively easy. Future case studies will be conducted in different regions to clarify the scope and limitations of the methodology used in this study and to explore its application to a wide range of slope hazard assessments for increased rainfall due to climate change.

References

1. Kaneko M (2018) Comprehending the landslide plale and residual strength of the re-slide type landslide, and the result of the slope stability analysis. A collection of papers from the China Branch of Geotechnical Society, pp 161–168
2. The Landslide Engineering Society of Japan Tohoku Branch (2001) Method for determining strength constants for landslide stability analysis, pp 99–110
3. Mima K (2007) Stability analysis method for ensuring safety during construction of landslide terminus cuttings. In: The 42nd geotechnical engineering research meeting of geotechnical society (Nagoya, Japan), pp 1931–1932
4. Yoshimatsu Y (1995) 3-D slope stability analysis of landslides (modified Hovland method)
5. Kosaka N (1982) Quasi-3-D infiltration analysis of wide-area groundwater by finite element method. JSCE Annual Academic Lecture Summary, Part 3:531–532
6. Iwai S (1970) Applied hydrodynamic statistics. Morikita Publishing Co, Chiyoda-ku, Tokyo
7. Ohtsuka S (2004) Slope stability analysis considering seepage property of slope. In: JSCE proceedings of the second symposium on landslides, pp 165–170